BIOCHEMISTRY
including biophysical chemistry & molecular biology

Article

pubs.acs.org/biochemistry

A Systematic Evaluation of Protein Kinase A−A-Kinase Anchoring Protein Interaction Motifs

Pepijn P. Burgers,[†,‡] Marcel A. G. van der Heyden,[§] Bart Kok,[§] Albert J. R. Heck,[†,‡] and Arjen Scholten*[,†,‡]

[†]Biomolecular Mass Spectrometry and Proteomics, Bijvoet Center for Biomolecular Research and Utrecht Institute for Pharmaceutical Sciences, Utrecht University, Padualaan 8, 3584 CH Utrecht, The Netherlands

[‡]Netherlands Proteomics Centre, Padualaan 8, 3584 CH Utrecht, The Netherlands

[§]Department of Medical Physiology, Division of Heart and Lungs, University Medical Centre Utrecht, Yalelaan 50, 3584 CM Utrecht, The Netherlands

S *Supporting Information*

ABSTRACT: Protein kinase A (PKA) in vertebrates is localized to specific locations in the cell via A-kinase anchoring proteins (AKAPs). The regulatory subunits of the four PKA isoforms (RIα, RIβ, RIIα, and RIIβ) each form a homodimer, and their dimerization domain interacts with a small helical region present in each of the more than 40 AKAPs reported so far. This allows for tight anchoring of PKA and efficient communication with other signaling proteins that interact with the AKAP scaffold in a spatial and temporal manner. The hydrophobic interaction surfaces of the PKA-R dimer and several AKAP helices have been investigated in great detail. Despite this knowledge, not every suggested AKAP has had its binding motif specified. Here we created an efficient bioinformatic tool, termed THAHIT, to accurately map the PKA binding motif and/or additional motifs of all previously reported AKAPs. Moreover, THAHIT predicts its specificity toward PKA-RIα and/or PKA-RIIα binding. To verify the validity of these newly predicted anchoring sites and their putative specificities, we used computational modeling approaches (HADDOCK), biochemical affinity studies (fluorescence anisotropy), and cellular colocalization studies. We further demonstrate the potential of THAHIT to identify novel AKAPs in cAMP-based chemical proteomics discovery data sets, and the human proteome. We retrieved numerous novel AKAP candidates, including a never reported 330 kDa AKAP observed in heart tissue, which we further characterized biochemically as a PKA-RIIα binder. Altogether, THAHIT provides a comprehensive overview of known and novel PKA−AKAP interaction domains and their PKA-R specificities.

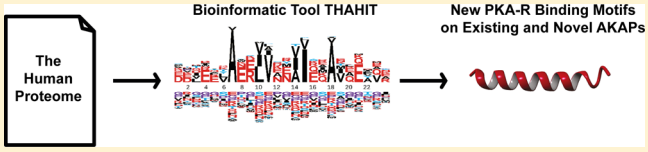

Many cellular processes, such as cell proliferation[1] and remodeling of the actin cytoskeleton,[2] are regulated via spatially and temporally segregated cAMP signaling pathways. A key component in these pathways is the cAMP-dependent protein kinase also known as protein kinase A (PKA).[3] PKA is a heterotetrameric kinase consisting of a regulatory subunit (PKA-R) dimer with each subunit binding to a catalytic (PKA-C) subunit.[4] There are four, genetically distinct, PKA-R isoforms (PKA-RIα and -β and PKA-RIIα and -β) and three PKA-C isoforms (α, β, and γ). Early on, cAMP and PKA were thought to diffuse freely throughout the cell. However, in 1982, the first A-kinase anchoring protein (AKAP), microtubule-associated protein (MAP2),[5,6] was reported, and since then, many more followed to currently comprise a family of more than 40 unique AKAP genes.[7,8] Many of these also include alternative splicing variants, expanding the family to more than 70 different protein species. AKAPs bind to PKA with high affinity and sequester it to a specific location inside the cell, close to a localized pool of cAMP and a specific set of substrates. Along with PKA, the AKAPs often tether many other signaling proteins, such as adenylate cyclases, phosphodiesterases, phosphatases, and other kinases. In this way, a very efficient signaling hub is created that is regulated in both space and time to allow segregation of the functionally distinct cAMP-regulated pathways.[7]

The first wave of AKAPs was identified by a method called the RII overlay.[9] This methodology was less successful using PKA-RI, and therefore, all "early" AKAPs were reported to have PKA-RII specificity. Later, in the 1990s using a two-hybrid screen, the first dual-specific AKAPs, dAKAP1 and dAKAP2, were revealed, which bind both PKA-RI and PKA-RII isoforms.[10,11] The capturing of AKAPs via binding of PKA-R to immobilized cAMP, the cAMP pull-down, is also frequently used today.[12,13] The AKAPs are then identified via Western blotting and/or mass spectrometry. This methodology led to the recent discovery of the first PKA-RI-specific AKAPs, sphingosine kinase type 1 interaction protein (SPHKAP) and small membrane AKAP (smAKAP).[14−16] Other methodologies used include the T7 phage display for discovering chromodomain helicase binding protein 8 and bioinformatics with follow-

Special Issue: New Frontiers in Kinases

Received: June 10, 2014
Revised: July 30, 2014
Published: August 6, 2014

   dx.doi.org/10.1021/bi500721a | *Biochemistry* 2015, 54, 11−21

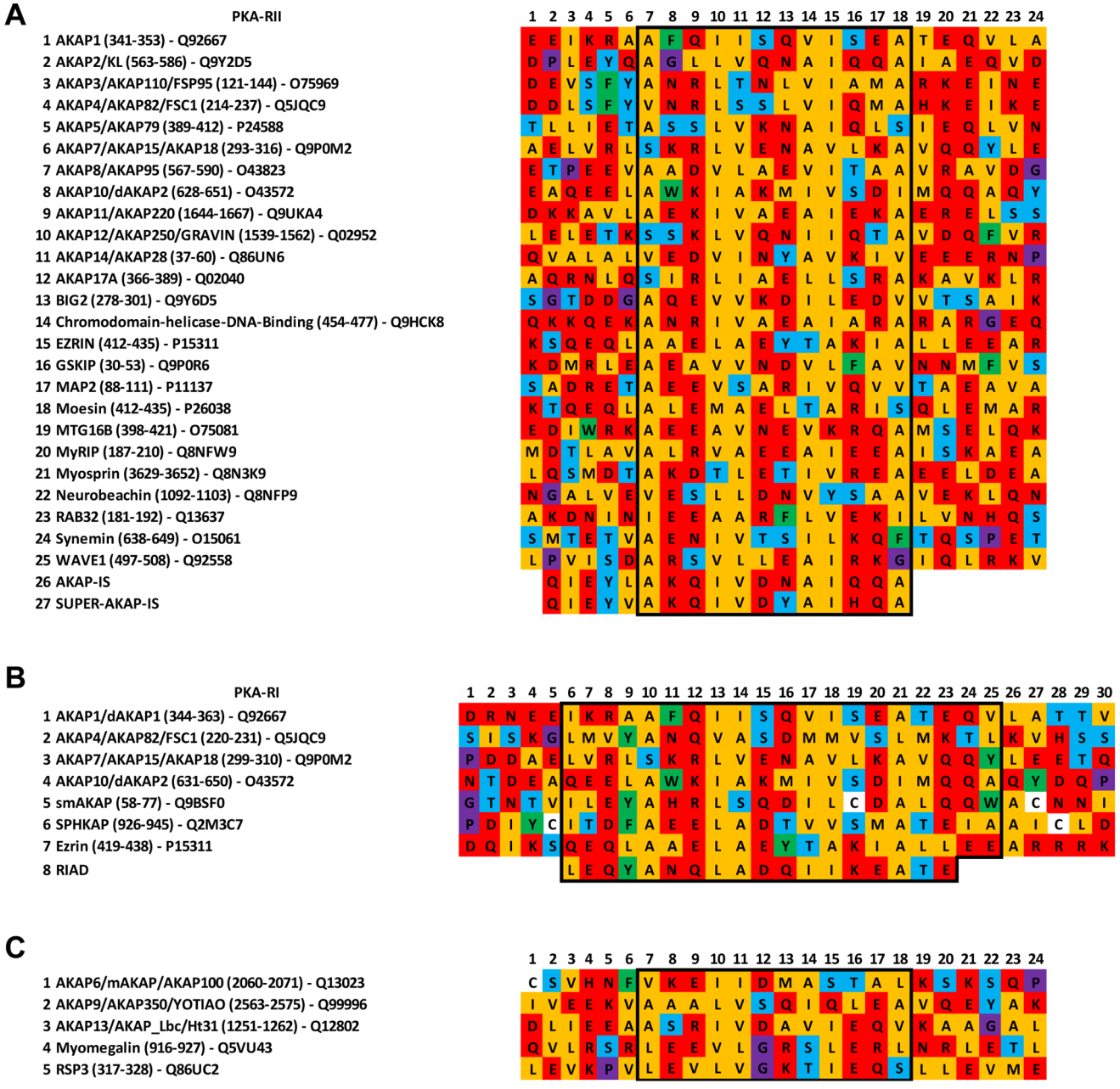

Figure 1. Alignments of PKA-R binding domain helices. Aligned in panel A are all known PKA-RIIα binding domains with substantial evidence of their genuineness. The residues are color-coded as follows: orange for aliphatic, red for polar, blue for S/T, green for bulky, and purple for G/P. Aligned in panel B are all known PKA-RIα binding domains (exhibiting substantial evidence of their genuineness) with similar color coding as described above. (C) THAHIT provides evidence of the identification of binding domains in AKAPs that had no previous substantial evidence of their PKA-R binding domain.

up studies to discover glycogen synthase kinase 3β interacting protein (GSKIP) as AKAPs.[17,18]

Carr et al. described the AKAP domain responsible for the high-affinity interaction between PKA and AKAPs for the first time.[19] The domain consists of a three- to four-turn amphipathic helix that uses its hydrophobic edge to dock to the dimerization/docking (D/D) domain of PKA.[20] Each AKAP has one or more amphipathic α-helices, which bind to the regulatory subunit dimer. Several structural studies have elucidated meticulous molecular detail on the interaction between PKA-RIα and PKA-RIIα with different AKAP helices by means of, for instance, crystal and NMR structures, mutation analyses, and peptide arrays.[21−24] The D/D domain of PKA-R consists of an X type four-helix bundle with a hydrophobic docking surface for the hydrophobic side of AKAP kinase binding domains.[20] There is a larger interaction surface present on PKA-RIαD/D than on PKA-RIIαD/D, which causes more restrictions on binding for PKA-RI-interacting AKAPs.[21]

The most common means of initially attempting to locate the PKA binding domain is via determining the presence of an amphipathic helix using bioinformatics tools. Afterward, there are several options to validate these findings, with pros and cons to each, such as peptide arrays,[24] amino acid substitutions (with proline as a helix disruptor being the common choice), deletion mapping combined with Western blotting, colocalization studies or Co-IPs, and studies of the binding affinity

dx.doi.org/10.1021/bi500721a | *Biochemistry* 2015, 54, 11−21

between the predicted domain and PKA-R. By means of these various studies, many of the PKA-RIIα and PKA-RIα binding domains have been confirmed. However, not every report of a novel AKAP in the literature has presented the interaction region with equal detail and evidence.

On the basis of a data set of previously confirmed amphipathic helices recorded with confidence, we developed here a software tool, THAHIT (the AKAP/amphipathic helix identification tool), to identify PKA binding domains based upon various stringent structural factors. THAHIT proves to be a versatile software tool for predicting and specifying existing, but more importantly, also novel AKAP−PKA anchoring domains, and here we present the first comprehensive overview of all PKA−AKAP interaction domains and their putative specificity.

EXPERIMENTAL PROCEDURES

Development of THAHIT. The software tool was written in Python and makes use of Biopython version 1.62, NetSurfP for secondary structure predictions, and an evolutionary conservation analysis previously published.[25]

Cell Culture. HEK293 cells were sustained in Dulbecco's modified Eagle's medium (Lonza, Basel, Switzerland) containing 10% heat-inactivated fetal bovine serum (Lonza) and glutamine (Lonza) in 35 mm glass bottom dishes (MatTek). The dishes for imaging were coated with poly-D-lysine. Cells were grown to 75% confluence and transfected with the plasmids (WAVE2-GFP, WAVE2ΔC-GFP, and PKA-RIIα-mCherry) using PolyFect according to the manufacturer's protocol for the specific cell type (Qiagen).

Protein and Peptide Synthesis. Seven peptides (WAVE1 amino acids 20−43, RGIKNELECVTNISLANIIRQLSS; *vl*AKAP amino acids 1299−1322, CLLEDKARELVNEIIYVAQEKLRN; AKAP7γ amino acids 294−317, AELVRLSKRLVENAVLKAVQQYLE; Ezrin amino acids 84−107, FYPEDVAEELIQDITQKLFFLQVK; AKAP10 amino acids 629−652, EAQEELAWKIAKMIVSDIMQQAQY; RIAD, TVLEQYANQLADQIIKEATE; and superAKAP-IS, QIEYVAKQIVDYAIHQA) were synthesized and purified to ∼95% (NKI). The peptides were N-terminally tagged with 5-TAMRA. Full-length PKA-RIα and PKA-RIIα dimers were purified as described previously.[26]

Fluorescence Anisotropy. Measurements were taken with the PHERAstar microplate reader (BMG LABTECH GmbH) using the FP module with excitation at 540 nm and emission at 590 nm. Flat bottom black 96-well plates (Thermo) were used. The concentration of each AKAP peptide was 1 nM, whereas the concentration of PKA ranged from 0.01 to 2000 nM depending upon the binding affinity of each individual peptide. The buffer consisted of 50 mM NaCl and 25 mM Tris (pH 7.4). Each of the binding experiments was conducted four times at room temperature. Then the data were put into the nonlinear regression model of one-site saturated binding in GraphPad Prism 5.0.

Fluorescence Imaging. Cells were washed once with ice-cold PBS, fixed in 4% ice-cold formaldehyde in PBS, and then washed twice with PBS. The confocal images were obtained with a Zeiss LSM700 confocal system with a 63× oil objective lens.

Statistics and Quantification. The two fluorescence profiles were compared with ImageJ 1.43 by plotting a line through the visible cell and then creating a plot profile. The profiles were compared, and an R^2 correlation coefficient was computed using MS Excel.

Reverse Transcription Polymerase Chain Reaction (RT-PCR). Total RNAs of brain, skeletal muscle, ventricle, stomach, spleen, liver, kidney, lung, ovary, and testicle were isolated from a female rat using TRIzol reagent (Invitrogen). Afterward, the RNAs were treated with DNaseI followed by addition of oligo$(dT)_{12}$-VN (Promega) and Superscript II (Invitrogen). Finally, the PCR was completed using *Taq* polymerase (Invitrogen) and the appropriate primers (Eurogentec) for rat *vl*AKAP and rat GAPDH.

RESULTS

Foundations of the AKAP/Amphipathic Helix Identification Tool (THAHIT). To build THAHIT, two comprehensive lists of all known human PKA-RIα- and PKA-RIIα-specific AKAPs were gathered.[5,9,10,15−18,27−59] From these, the amphipathic helices were selected on the basis of stringent validation criteria using information in the literature to create two high-confidence amphipathic helix collections. Solely sequences confirmed by multiple biochemical assays (deletion, mutation, proline substitution, etc.) were used for THAHIT. These sequences were manually aligned on the basis of the knowledge of crystal and NMR structures, peptide array data, and binding affinity data (Figure 1A,B). The alignments were color-coded, and the amphipathic binding motifs revealed themselves by the alternating yellow and red colors representing the hydrophobic and hydrophilic amino acids, respectively. The appropriate parameters for the identification of more PKA-RII binding domains were extracted from these alignments. Previous AKAP motif search tools mostly paid attention to the hydrophobic side of the helix,[18] but accumulating structural evidence also suggests a role for some of the hydrophilic residues in the interaction.[24] Therefore, we incorporated sequence requirements for both sides of the amphipathic helix. The hydrophilic surface is important in that it is largely a nonburied surface. Thus, it is mostly in contact with water and therefore prefers polar residues. The hydrophobic domain requires the following 12-residue motif: [A/V/L/I/S]-X-X-[A/V/L/I]-[A/V/L/I/S/T]-X-X-[A/V/L/I/S/T]-[A/V/L/I]-X-X-[A/V/L/I/S]. The hydrophilic domain (X) requires a minimum of three X's to consist of H/R/K/D/E/N/Q (residues colored red in sequence alignments) or two plus at least one S/T. For additional stringency, for the 12-residue motif a minimal helix propensity score of 70% was demanded.[60] No proline residue is permitted within this entire motif or at least three residues downstream and at least one residue upstream of the motif as this strongly disturbs the helix propensity. Only one glycine is allowed to be present inside the helix motif as more than one will severely disturb the helicity. Furthermore, one cysteine is permitted within the entire motif or at least one residue upstream or downstream of the motif. A pI value range of 3.3−6.25, which was previously used in a bioinformatics motif search for novel AKAPs, was applied to the motif.[18] Searches were conducted by screening 24-mer sequences one residue at a time, throughout each protein. As an additional quality filter, we used evolutionary conservation. For this, we compared the helical motif throughout species allowing only variants that still obey the human motif described above. We aligned the amphipathic helices with their homologues in chimpanzee, cow, mouse, and zebrafish, and only sequences stringently conserved from human to mouse were accepted.

dx.doi.org/10.1021/bi500721a | *Biochemistry* 2015, 54, 11−21

The approach mentioned above was also used to extract a motif from the PKA-RIα helix alignments. This resulted in a longer 18-residue motif (Figure 1B), X-X-[A/L/F/Y]-[A/L/I]-X-X-[L/V/I]-[A/V/I/S]-X-X-[A/V/I/T/M]-[A/V/L/I/T/M]-X-X-[A/L/I]-[V/L/T/M/H]-X-X, in which at least seven X's consist of H/R/K/D/E/N/Q. The same helix propensity parameters are inferred. No proline was allowed inside the motif or one residue downstream, whereas there were no glycine residues and only one cysteine residue allowed from position 2 to 18 in the motif plus one downstream. Searches were conducted by screening 30-mer peptides one residue at a time throughout each protein.

Identification and Verification of Amphipathic Helices. To assess the functionality of THAHIT, we used it on the entire human proteome (Uniprot database 2013-02; taxonomy, *Homo sapiens*). THAHIT subdivided the hits and aligned the PKA-RIα and PKA-RIIα binding helices. This resulted in 849 PKA-RIIα motifs found in 723 proteins (Table 1 of the Supporting Information). Of these, 387 sequences (348 proteins) are conserved from human to zebrafish, leaving the 462 remaining sequences dating back only to mouse. All these motifs were then put into MAST (MEME) to quantify the goodness of fit to the human model in panels A and B of Figure 1. These were used to rank the hits starting with the best. As expected, among the top-ranking motifs were many known AKAPs (Table 1 of the Supporting Information). THAHIT identified and specified almost all amphipathic helices used as input. Of the 25 high-confidence PKA-RIIα binding AKAP helices in Figure 1A, 21 were retrieved by THAHIT (84%). The ones not retrieved by THAHIT were AKAP17A, chromodomain-helicase-DNA-binding, MTG16B, and Neurobeachin. In addition, we could predict the exact binding sequences of AKAPs for which the biochemical validation did not meet the criteria stated above (Figure 1C). For instance, the exact amphipathic helices of myomegalin[48] and RSP3[56] were for the first time pinpointed by THAHIT. Also, on several AKAPs reported in the literature without a specified helix, we were not able to define a likely helix motif (e.g., for pericentrin, α4-integrin, and MyosinV and -VIIa), suggesting these proteins may possibly interact with PKA via an alternative mechanism. All results were manually scrutinized against the published data. Interestingly, without the application of the pI and conservation parameters, there was a list of only 28 PKA-RIα motifs [25 proteins (Table 2 of the Supporting Information)]. All of the PKA-RI binding peptides used to build the model were retrieved by THAHIT. These included the well-known dual-specific AKAP1 and AKAP10 as well as the RI-specific SPHKAP and smAKAP. In both lists, we retrieved protein hits with high MAST scores not previously annotated as AKAPs. For instance, Golgi SNAP receptor complex member 1 that is bound to the Golgi membrane[61] is predicted to be a strong PKA-RIIα binding AKAP. Hexokinase-1, an allosteric enzyme inhibited by its product Glc-6-P,[62] on the other hand is predicted to be a strong PKA-RIα binding AKAP. These plead for further experimental validation.

An Improved Model of RI and RII Amphipathic Helices. We then aligned the amphipathic helix sequences of all reported AKAPs from the literature and those identified and/or confirmed via THAHIT using pLogo based on the binding preference. A highly conserved motif was created for both the PKA-RIα and PKA-RIIα binding domains (Figure 2A,B). The PKA-RIIα motif is much more defined, likely as there is a larger set of established PKA-RIIα binding AKAPs

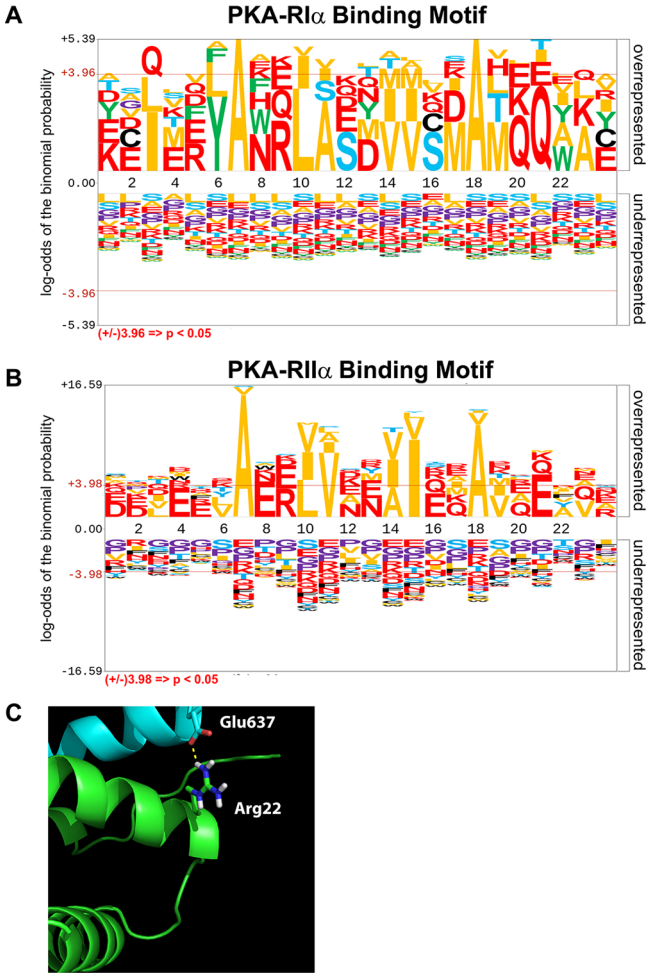

Figure 2. Using all helix sequences depicted in Figure 1, a higher-definition amphipathic helix motif was created using pLogo. Motifs of the PKA-RIα and PKA-RIIα binding amphipathic helices are depicted in panels A and B, respectively. (C) HADDOCK-based docking structure of d-AKAP2 and PKA-RIIα. Shown is the interaction between the previously not annotated conserved polar residue at position 4 (Glu637) of the helix (see A) and Arg22 of PKA-RIIα that interact and thus play a role in PKA–AKAP affinity.

(Figure 2A). In the PKA-RII motif, the central double hydrophobic residues stand out (positions 10 and 11 and positions 14 and 15). A double hydrophobic residue seems less important at the flanking regions where alanine residues at positions 7 and 18 seem to suffice. Besides these detailed motif elements, we discovered a clear consensus of polar residues three residues upstream of Ala7 (position 4) and downstream of Ala18 (position 21). Notably, 23 of a total of 32 AKAP sequences have a polar residue at position 4, and at position 21, this is 23 of 30 (this includes synthetic peptides AKAP-*IS* and superAKAP-*IS* that do not contain the C-terminus). Among these, there seems to be a strong preference for glutamic acid (11 of 23 at both positions 4 and 21). This was thus far not recognized; therefore, we set out to investigate the nature of this additional hydrophilic region. We used molecular docking studies with HADDOCK[63,64] to elucidate the potential interactions of these polar residues. HADDOCK gives a score to a model based upon electrostatic energy, van der Waals energy, desolvation energy, and restraint violation energies. The crystal structure of PKA-RIIα's D/D-domain and the amphipathic helix of dAKAP2 revealed that Glu631 can form

dx.doi.org/10.1021/bi500721a | *Biochemistry* 2015, 54, 11−21

Table 1. Additional PKA-RIα and PKA-RIIα Binding Domains Predicted by THAHIT for Established AKAPs

AKAP	region	PKA-RIα	PKA-RIIα
AKAP3	287−300	YANSVVSDMMVSIM	
AKAP6	1624−1635		VGELSKRTLDLL
AKAP11	619−630		VSEALSNALKDL
AKAP11	689−700		AKDLSESVIQEA
AKAP12	1366−1377		SEEVSKQLLQTV
Ezrin	88−101	VAELLIQDITQKLF	
Moesin	88−101	VSEELIQDITQRLF	
Neurobeachin	480−491		VKAIVTHSIHSA
WAVE1	25−36		LECVTNISLANI

a hydrogen bridge with Arg22 of PKA-RIIα (Figure 2C), supporting its conserved importance at the PKA-RII−AKAP interface.

New Helices on Old AKAPs. For several AKAPs, such as AKAP4,[29] SPHKAP,[16] and AKAP11,[36] multiple PKA binding domains have been identified, and these were all also found using THAHIT. We hypothesized that other AKAPs may also contain additional, currently overlooked, binding sites. In our analysis, THAHIT recognized in total 11 novel additional PKA-RIα and/or PKA-RIIα binding sites on 10 different AKAPs (Table 1). For instance, THAHIT suggested an additional PKA-RIα/PKA-RIIα binding domain at the N-terminus (amino acids 84−107) of Ezrin (another dual-specific anchoring domain was already annotated via Co-IPs at the C-terminus, amino acids 412−435[44]). Also, an additional PKA-RII binding domain at the N-terminus (amino acids 20−43) of Wiskott-Aldrich syndrome protein family member 1 (WAVE1) was observed. To confirm the validity of these newly predicted PKA binding domains, we performed biochemical validation experiments as described in more detail below.

Ezrin. The novel PKA binding domain of Ezrin (amino acids 84−107) as extracted from the sequence by THAHIT is 100% conserved from human to zebrafish (Figure 3). To further

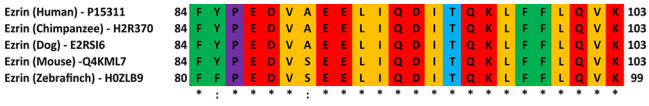

Figure 3. Conservation of the putative PKA-RIα/PKA-RIIα binding domain of Ezrin (amino acids 88−102) extracted by THAHIT. Using ClustalW, the domain was aligned and showed 100% conservation in a wide range of species (human, chimpanzee, cow, mouse, and zebrafinch).

investigate this putative binding site, we first used modeling by HADDOCK on a set of crystal structures available for the PKA-RIα and PKA-RIIα D/D domain binding to several different AKAP amphipathic helix peptides.[63,64] By comparing the HADDOCK scores of different (putative) AKAP helices docking onto the two PKA-R structures, we aimed to evaluate goodness of fit for the domains predicted by THAHIT. We used several known models as internal calibrants. The affinities and PKA-R specificities of these are known. We chose superAKAP-IS (PKA-RIIα-specific), smAKAP (PKA-RIα-specific), AKAP10 (dual-specific), and AKAP7 (amino acids 294−317, strong RII, modest RI binding) as they present various affinities and specificities toward PKA-RIα and RIIα. Scrambled peptides were used as negative controls. The final HADDOCK structures were qualitatively inspected on the basis of positioning and helicity. We found that the novel Ezrin (amino acids 84−107) domain docked better onto PKA-RIα than AKAP7 and the scrambled peptide but had a poorer HADDOCK score than RI-specific smAKAP and dual-specific AKAP10 (Table 2), suggesting it also is a dual-specific site. Therefore, we also performed binding predictions with the PKA-RIIα structure (Table 2). We observed a remarkably strong score for AKAP7, which was even better than that of the engineered RII-specific sequence of superAKAP-IS. The new domain in Ezrin scored poorer than AKAP7 and AKAP10 but still had a score better than that of the scrambled peptide. To confirm these *in silico* results, we measured the actual affinities using fluorescence anisotropy binding studies with full-length recombinant PKA-RIα, PKA-RIIα, and synthetic peptides of the different amphipathic helices tagged with 5-TAMRA. The novel amphipathic helix of Ezrin had a K_d of 78 ± 8.5 nM for PKA-RIα compared to AKAP7 that had a K_d of 119 ± 12 nM, whereas AKAP10, smAKAP, and RIAD presented K_d values of 9.4 ± 0.8, 4.3 ± 0.4, and 2.0 ± 0.2 nM, respectively (Figure 4).

Table 2. Evaluation of Specificity by Molecular Modeling[a]

AKAP	PKA-RIα	PKA-RIIα
smAKAP (amino acids 56−79)	−139.8 ± 3.5	–
superAKAP-IS	–	−83.7 ± 14.4
AKAP7γ (amino acids 294−317)	−110.1 ± 2.0	−91.3 ± 3.0
AKAP10 (amino acids 629−652)	−126.1 ± 1.7	−82.8 ± 1.1
Ezrin (amino acids 84−107)	−120.7 ± 8.0	−72.3 ± 2.4
WAVE1/WAVE2 (amino acids 20−43)	–	−85.4 ± 4.5
*vl*AKAP (amino acids 1299−1322)	–	−82.5 ± 1.7
hexokinase-1 (amino acids 21−44)	−140.7 ± 6.3	–
28 kDa Golgi SNARE protein (amino acids 167−190)	–	−81.3 ± 3.4
scrambled	−83.1 ± 3.4	−54.7 ± 4.8

[a]HADDOCK scores of various PKA-R binding domain peptides docking onto PKA-RIα and PKA-RIIα. A dash means the value was not acquired. The lower the score, the stronger the interaction.

dx.doi.org/10.1021/bi500721a | *Biochemistry* 2015, 54, 11−21

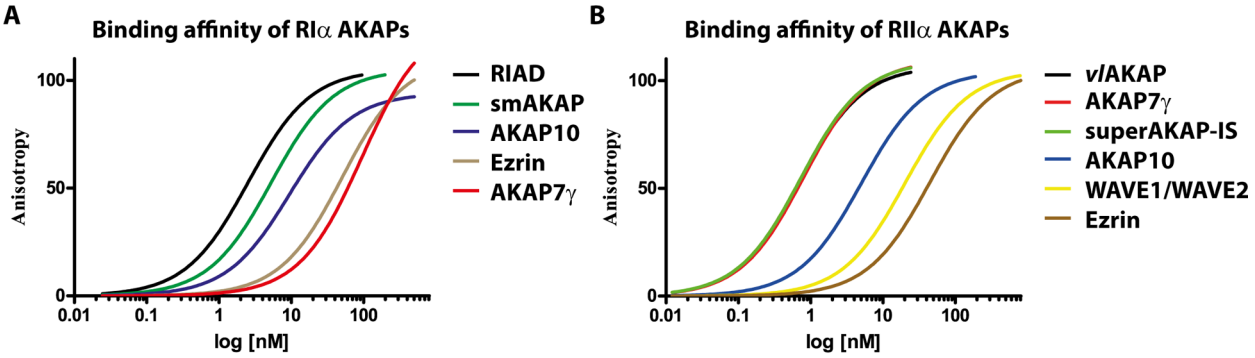

C

AKAP	PKA-RIα (nM)	PKA-RIIα (nM)
smAKAP(AA56-79)	4.3 ± 0.4	-
superAKAP-IS	-	0.6 ± 0.1
AKAP7γ (AA294-317)	119 ± 12.0	0.6 ± 0.1
AKAP10 (AA629-652)	9.4 ± 0.8	4.3 ± 0.3
Ezrin (AA84-107)	78 ± 8.5	32 ± 2.8
WAVE1/WAVE2 (AA20-43)	-	20 ± 1.3
*vl*AKAP (AA1299-1322)	>1000	0.7 ± 0.1
RIAD	2.0 ± 0.2	-
Scrambled	>1000	>1000

Figure 4. Assessing PKA−AKAP interactions by fluorescence binding assays. The same set of PKA-R binding domain peptides from Table 2 were synthesized with a 5-TAMRA tag attached. Using fluorescence anisotropy, the binding affinities were measured between these AKAP mimicking peptides and PKA-RIα/PKA-RIIα. (A and B) Dose−response curves of each PKA−AKAP interaction (with the exception of a binding affinity of >1000 nM). (C) Binding affinities (n = 4) of both the PKA-RIα and PKA-RIIα binding AKAPs (a dash means not measured).

This novel Ezrin site also interacts with PKA-RIIα, reiterating it is a dual-specific site (K_d = 32 ± 2.8 nM). This affinity was lower than that exhibited by the peptides originating from superAKAP-IS, AKAP7, and AKAP10 but still 3 orders better than that of the scrambled peptide (Figure 4). This confirms THAHIT's prediction that Ezrin has not only a PKA-RIα/PKA-RIIα binding domain at the C-terminus but also an additional one at the N-terminus. Additionally, it confirms that THAHIT has the ability to properly predict PKA-RIα binding motifs.

WAVE1/WAVE2. Interestingly, WAVE1 is a validated AKAP for which a PKA-RIIα binding domain has been annotated via deletion mapping and Co-IPs at the C-terminus (amino acids 491−514).[58] WAVE1−WAVE3 seem very homologous in this C-terminal region (Figure 5A), but an important difference is present within the amphipathic helix, where a crucial hydrophobic amino acid (V500) in WAVE1 is substituted with an aspartic acid (D439), which hampers PKA binding. The original WAVE1 study provided experimental evidence (RII overlay and Co-IP with PKA-C) corroborating that the C-termini of WAVE2 and WAVE3 do not have PKA-RII binding capabilities, and therefore, these two proteins were not considered as AKAPs. However, THAHIT also predicts a novel RII binding region at the N-terminus of WAVE1 (Table 1 and Figure 5B). THAHIT's suggested PKA-RIIα binding domain of WAVE1 is well conserved from human to zebrafish (Figure 5C). Interestingly, the human WAVE2 has the exact same N-terminal binding motif as WAVE1. However, it was not recognized by THAHIT because of the conservation module as the mouse species has one key mutation (several other species such as cat and dog on the other hand do not carry that critical mutation) (Figure 5C). Using WAVE2 as a representative, we performed HADDOCK and fluorescence anisotropy studies. PKA-RIIα HADDOCK binding studies of the WAVE1/WAVE2 N-terminal putative amphipathic helix were again used to compare to the control set used for Ezrin. The WAVE1/WAVE2 peptide had a score slightly poorer than that of superAKAP-IS and a bit better than that of AKAP10 but a result much better than that of the scrambled peptide (Table 2). The actual affinities we acquired by fluorescence anisotropy reflected the modeling data perfectly; AKAP7 showed a binding affinity (K_d = 0.6 ± 0.1 nM) as strong as that of superAKAP-IS (K_d = 0.6 ± 0.1 nM) for PKA-RIIα. WAVE1/WAVE2 had a binding affinity (K_d = 20 ± 1.3 nM) weaker than that of AKAP10 (K_d = 4.3 ± 0.3 nM) (Figure 4). As mentioned, WAVE2 was initially not thought to have a PKA-RIIα binding domain and therefore not to be an AKAP.[58] To further validate whether WAVE2 is indeed an AKAP via this N-terminal region, we performed a colocalization study using a full-length WAVE2-GFP construct and a WAVE2 construct lacking the C-terminal amphipathic helix (WAVE2ΔC-GFP). Confocal microscopy showed that WAVE2ΔC-GFP, which contains only the N-terminal amphipathic helix, also colocalizes with PKA-RIIα-mCherry and can thus act as an AKAP *in situ* (Figure 5D,E).

THAHIT Identifies a Novel AKAP, *vl*AKAP. As outlined above, several putative AKAPs not previously annotated were retrieved from the human proteome by THAHIT. In particular for PKA-RII, the list is rather extensive. To verify the validity of these hits, we applied THAHIT to proteins which were affinity purified by cAMP-based chemical proteomics, a method that we earlier successfully used to identify novel AKAPs in cells and tissues.[14,65,66] When screening the data used in the identification of smAKAP[14] in human platelets and heart tissue, THAHIT readily identified smAKAP with the appropriate prediction for PKA-RIα binding. When screening the identifications from other cAMP-based chemical proteomics experiments performed in rat and mouse heart,[65,66] in which we identified SPHKAP for the first time, we encountered an

dx.doi.org/10.1021/bi500721a | *Biochemistry* 2015, 54, 11−21

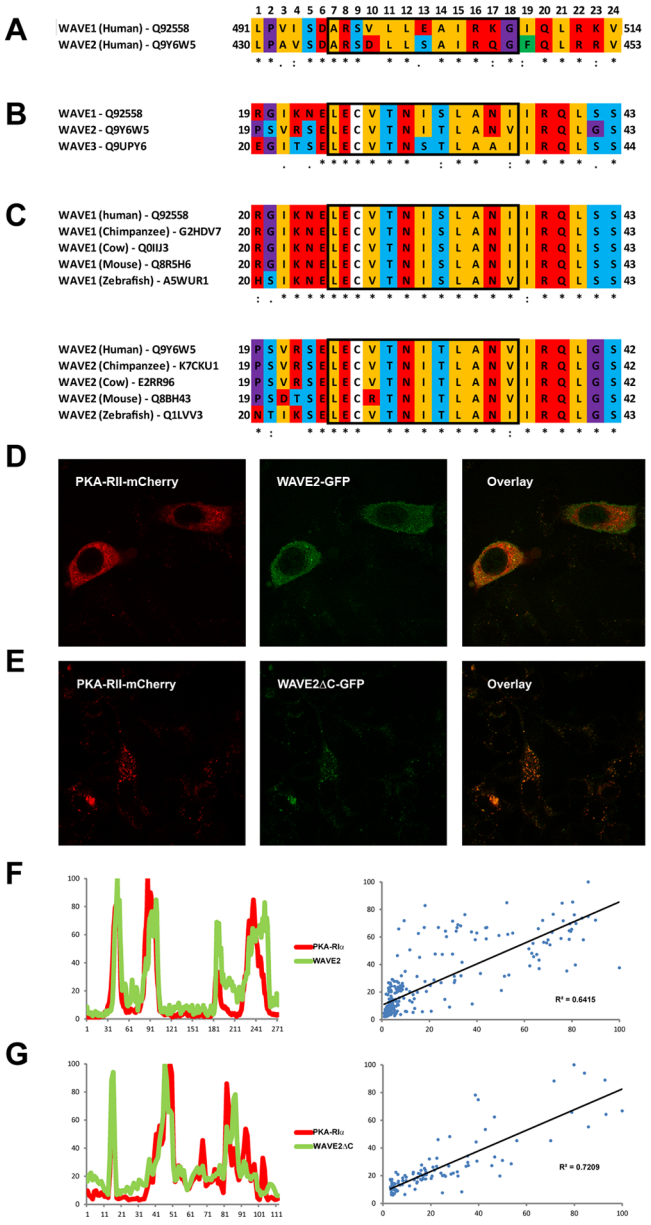

Figure 5. Characterizing the WAVE PKA-RIIα N-terminal binding domain. (A) Sequence alignment of the known PKA-RIIα C-terminal binding domain of WAVE1 with its isoform WAVE2. (B) Sequence alignment of THAHIT's proposed N-terminal PKA-RIIα binding domains of WAVE1−WAVE3. (C) Sequence conservation of the putative N-terminal amphipathic helices of WAVE1 (amino acids 25−36) and WAVE2 (amino acids 25−36) using ClustalW over a wide range of species (human, chimpanzee, dog, mouse, and zebrafinch). (D) PKA-RIIα-mCherry and full-length WAVE2-GFP are both expressed in HEK293 cells. Confocal imaging shows the N-terminus of WAVE2 colocalizing with PKA-RIIα. (E) Additionally, in agreement with the data generated by THAHIT, HEK293 cells expressing PKA-RIIα-mCherry and WAVE2ΔC-GFP reveal colocalization of both proteins. For both panels D and E, a line plot profile and correlation analysis of colocalization was performed. The plot profiles display the difference in fluorescence intensity along a line taken through the cell. Scatter plots (far right) show the pixel distribution with which the R^2 was calculated.

unknown protein (IPI00370756, Human accession number XP_005247174.1, unverified UniProtKB protein B4DLE8) with a molecular mass of 330 kDa. Accoding to THAHIT, it contained a possible PKA-RIIα interacting helix between amino acids 1299 and 1322. We termed this protein, for which no function has been annotated, *vl*AKAP, for very large AKAP. As with the other AKAPs, the helix is very well conserved among different vertebrate species (Figure 6A). When added to THAHIT's proteome wide motif MAST score list, the motif of *vl*AKAP ranked 12th among all proteins and 3rd among unknown AKAPs. To confirm that this full-length protein is expressed in tissue, and not just the first 1365 residues as suggested by the UniProtKB (B4DLE8) database, we were able to match 14 peptide spectra (of the chemical proteomics data sets) spread along the entire rat protein (Figure 6B). These peptides were all identified in the same gel band in a high-molecular mass region on the one-dimensional gel above the 260 kDa marker. To investigate whether *vl*AKAP has more conserved domains, we performed a BLAST analysis. First, we checked for putative conserved domains in both the human and rat sequences. These were found only at the very C-terminus (Figure 6B,C). Between amino acids 2043 and 2092, 2138 and 2176, 2188 and 2232, 2233 and 2275, 2281 and 2322, 2323 and 2365, 2376 and 2412, 2413 and 2455, and 2502 and 2543, there are predicted β/γ crystallin domains for the human whereas the rat showed only five such domains at the N-terminus. Further downstream, at the very C-terminus between amino acids 2575 and 2677, there is a ricin B type lectin domain. The former domains were first only recognized as the major constituents of the vertebrate eye lens.[67] The ricin domain is described as a carbohydrate binding domain. We next evaluated the expression of *vl*AKAP across various rat tissues by means of mRNA RT-PCR. It was ubiquitously expressed, with the highest levels of expression in testicles, lungs, and skeletal muscle (Figure 6D). Again, we applied HADDOCK and fluorescence anisotropy studies to confirm the domain predicted by THAHIT further (amino acids 1299−1322). The HADDOCK results suggested a very strong binding affinity (score of -82.5 ± 1.7) comparing very well with those of other PKA-RII binding AKAPs (Table 2). The *in vitro* binding affinity studies further confirm this site with a K_d of 0.7 $\pm$ 0.1 nM for binding to PKA-RIIα, close to the value of the strongest RII binding AKAPs superAKAP-IS and AKAP7 (Figure 4). Thus, via THAHIT's screening of the chemical proteomics data sets and additional verification using conservation analysis, docking, and *in vitro* binding studies, we identified a novel PKA-RIIα binding AKAP, *vl*AKAP.

DISCUSSION

On the basis of available protein interaction data, we developed a bioinformatics tool termed the AKAP/amphipathic helix identification tool (THAHIT) to characterize the wide repertoire of proteins that interact with the regulatory subunits of protein kinase A. We show that THAHIT can identify and distinguish PKA-RIα and PKA-RIIα binding domains, as illustrated by the discovery of new helices on WAVE1/WAVE2 and Ezrin. In 2000, when WAVE1 was first identified as an AKAP via Co-IPs, it was shown that WAVE2 (and WAVE3 as well) did not coprecipitate with PKA and that only the C-terminus of WAVE1 could be pulled down by PKA-RIIα.[58] In contrast, another more recent study performed similar Co-IPs and did show coprecipitation of WAVE2 with PKA-RIIα.[59] This study did indeed find the N-terminus of WAVE2 binding PKA as well, the responsible helix was not further specified. Interestingly, a possible explanation for the differing Co-IP results is as follows. There is a crystal structure

dx.doi.org/10.1021/bi500721a | *Biochemistry* 2015, 54, 11−21

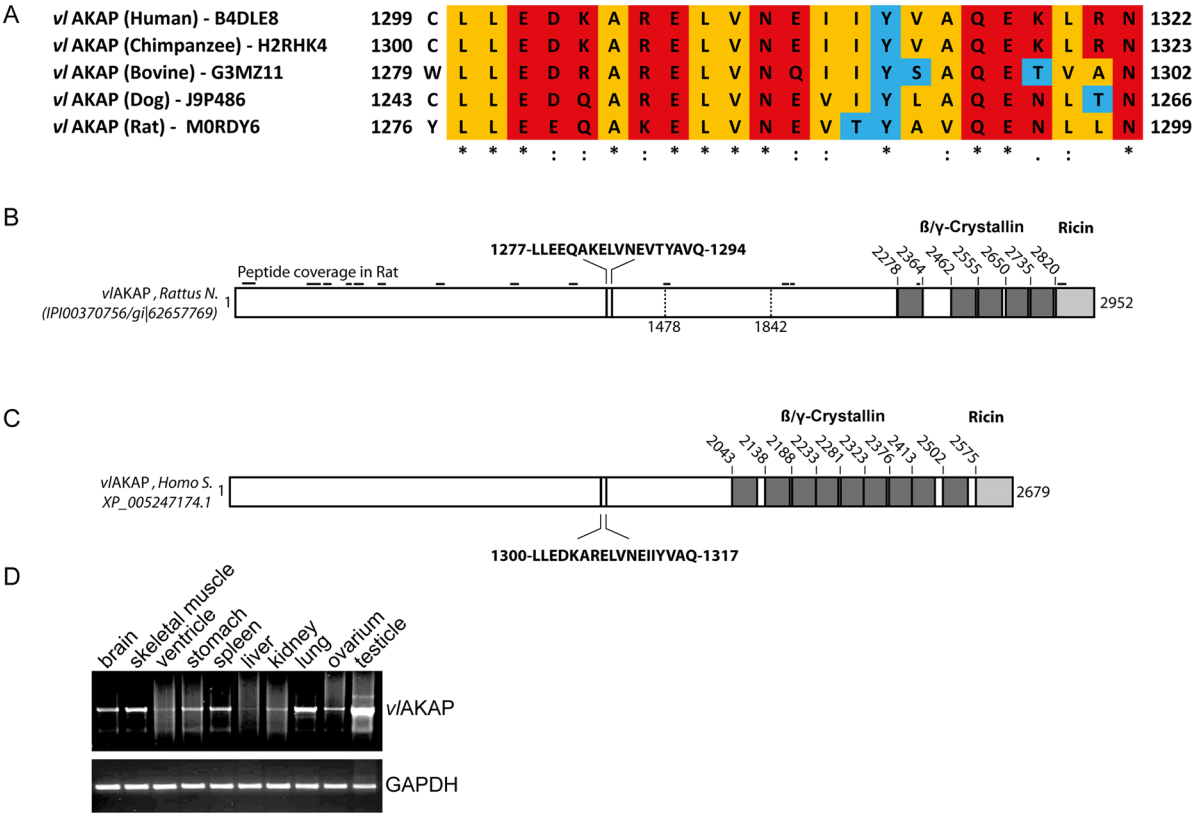

Figure 6. Characterizing the novel AKAP, *vl*AKAP, discovered via assessing chemical proteomic data sets using THAHIT. (A) Aligment of human, chimpanzee, bovine, dog, and rat *vl*AKAP PKA-RIIα binding domain sequences. (B) Rat *vl*AKAP, pulled down from rat ventricular tissue in a previous study[1] with the putative PKA-RII binding amphipathic helix depicted (amino acids 1277−1294). *vl*AKAP contains several β/γ crystallin domains (dark gray) at the C-terminus, as well as a ricin domain (light gray). At the top, the 14 identified unique peptides are depicted at their proper location in the sequence, consistent with the size of *vl*AKAP. (C) Human *vl*AKAP with the putative amphipathic helix depicted contains similar domains as identified in the rat species. (D) Semiquantitive RT-PCR analysis of *vl*AKAP in several tissues and organs of adult rats, based on amplification of a C-terminal 1335 bp fragment. Representative results of three independent experiments are shown. GAPDH was used as a control.

of the actin regulatory WAVE complex (Protein Data Bank entry 3P8C), which includes the N-terminal PKA-RIIα binding domain suggested here.[68] In the crystal structure, the PKA binding amphipathic helix is bound to Abl interactor 2. These data suggest that there are varying cellular conditions that prohibit or allow WAVE1 and WAVE2 to pull down PKA due to overlapping binding domains, thus displaying one of the cons of Co-IPs, false negatives. However, on the basis of these findings, we confirm WAVE1 and WAVE2 to have a PKA-RIIα binding domain at the N-terminus (amino acids 26−37 and 25−36, respectively). We suggest WAVE3 may contain a PKA-RIIα binding domain, as well, although its amphipathic helix is not as decent as those of WAVE1 and WAVE2 (Figure 4A and Table 2).

THAHIT did not assign a fitting amphipathic helix to every AKAP. This came as no surprise to us for the AKAPs α4 integrin[41] and pericentrin.[42] In the discovery manuscripts, pericentrin is described as requiring a domain stretching 100 residues to bind to PKA-RIIα, whereas α4 integrin binds directly to PKA-C and pulls down PKA-RIα via its catalytic subunit.[41,42] One may question if these AKAPs can be considered canonical or should maybe be considered as subclasses, as it seems that the PKA-R binding motif is much conserved throughout other AKAPs.

These examples illustrate the necessity of defining the PKA binding domain as narrowly as possible. Colocalization studies and/or IPs provide a good initial suggestion of interaction in the cellular context, but these do not distinguish between direct and indirect binding. To further evaluate this, binding affinity studies using fluorescence anisotropy,[14] surface plasmon resonance,[40,69] or isothermal calorimetry employed important complementary techniques that are ideally performed with full-length PKA-R and well-recognized PKA-R binding domains as controls. Another method for confirming the binding domain is a peptide array, as performed with MyRIP,[52] although the three-dimensional structure of the AKAP is likely compromised. Ideally, a complementary set of methods is used to provide sufficient evidence of the direct PKA-R−AKAP interaction under study.

To conclude, THAHIT helped us create an improved understanding and clearer picture of the PKA binding motifs of AKAPs, and we established the importance of additional hydrophilic interactions as novel binding parameters. Here we propose a list of new PKA-RIα and PKA-RIIα binding domains for existing AKAPs, suggesting that many AKAPs anchor more than one PKA enzyme. The exact nature of this curious observation is of high interest. Additionally, we have a list of possible (including known) PKA-RIIα motif proteins sorted by MAST score and a list of PKA-RIα motif proteins. This should make it easier to decide if a novel proposed AKAP is genuine. THAHIT also allowed us to unravel a novel AKAP, *vl*AKAP, while at the same time, it also led us to question some previously published AKAPs and their domains as this was not unambiguously defined for each AKAP. This should instigate

dx.doi.org/10.1021/bi500721a | *Biochemistry* 2015, 54, 11−21

the precise determination of the interaction surface between the PKA-R and AKAP in question via the suggested methods.

■ ASSOCIATED CONTENT

Supporting Information

Two supplementary tables containing the PKA-RIα and PKA-RIIα binding motifs discovered in the human proteome via THAHIT and ranked via MAST score. This material is available free of charge via the Internet at http://pubs.acs.org.

■ AUTHOR INFORMATION

Corresponding Author

*Telephone: +31302536793. Fax: +31302536919. E-mail: a.scholten@uu.nl.

Funding

This work was supported in part by the PRIME-XS Project, Grant 262067, funded by the European Union 7th Framework Programme. The Netherlands Proteomics Centre and The Netherlands Organization for Scientific Research (NWO), through funding the roadmap program *Proteins@Work* (Project 184.032.201), are acknowledged for support.

Notes

The authors declare no competing financial interest.

■ ACKNOWLEDGMENTS

We kindly thank Mao Peng for his assistance with the conservation analysis and Dr. Alexander Fish for his assistance with the fluorescence anisotropy measurements.

■ ABBREVIATIONS

AKAP, A-kinase anchoring protein; PKA, protein kinase A; RI and RII, regulatory subunits I and II, respectively; THAHIT, the Akap/amphipathic helix identification tool; GSKIP, glycogen synthase kinase 3β interacting protein; MAP2, microtubule-associated protein 2; SPHKAP, sphingosine kinase type 1 interaction protein; D/D, dimerization and docking domain; 5-TAMRA, 5-carboxytetramethylrhodamine; PKA-C, protein kinase A catalytic subunit; WAVE1, Wiskott-Aldrich syndrome protein family member 1.

■ REFERENCES

(1) Rodriguez, G., Ross, J. A., Nagy, Z. S., and Kirken, R. A. (2013) Forskolin-inducible cAMP pathway negatively regulates T-cell proliferation by uncoupling the interleukin-2 receptor complex. *J. Biol. Chem. 288*, 7137−7146.

(2) Hall, A. (1998) Rho GTPases and the actin cytoskeleton. *Science 279*, 509−514.

(3) Walsh, D. A., Perkins, J. P., and Krebs, E. G. (1968) An adenosine 3′,5′-monophosphate-dependant protein kinase from rabbit skeletal muscle. *J. Biol. Chem. 243*, 3763−3765.

(4) Krebs, E. G., and Beavo, J. A. (1979) Phosphorylation-dephosphorylation of enzymes. *Annu. Rev. Biochem. 48*, 923−959.

(5) Lohmann, S. M., DeCamilli, P., Einig, I., and Walter, U. (1984) High-affinity binding of the regulatory subunit (RII) of cAMP-dependent protein kinase to microtubule-associated and other cellular proteins. *Proc. Natl. Acad. Sci. U.S.A. 81*, 6723−6727.

(6) Theurkauf, W. E., and Vallee, R. B. (1982) Molecular characterization of the cAMP-dependent protein kinase bound to microtubule-associated protein 2. *J. Biol. Chem. 257*, 3284−3290.

(7) Welch, E. J., Jones, B. W., and Scott, J. D. (2010) Networking with AKAPs: Context-dependent regulation of anchored enzymes. *Mol. Interventions 10*, 86−97.

(8) Scholten, A., Aye, T. T., and Heck, A. J. (2008) A multi-angular mass spectrometric view at cyclic nucleotide dependent protein kinases: In vivo characterization and structure/function relationships. *Mass Spectrom. Rev. 27*, 331−353.

(9) Carr, D. W., Stofko-Hahn, R. E., Fraser, I. D., Cone, R. D., and Scott, J. D. (1992) Localization of the cAMP-dependent protein kinase to the postsynaptic densities by A-kinase anchoring proteins. Characterization of AKAP 79. *J. Biol. Chem. 267*, 16816−16823.

(10) Huang, L. J., Durick, K., Weiner, J. A., Chun, J., and Taylor, S. S. (1997) D-AKAP2, a novel protein kinase A anchoring protein with a putative RGS domain. *Proc. Natl. Acad. Sci. U.S.A. 94*, 11184−11189.

(11) Huang, L. J., Durick, K., Weiner, J. A., Chun, J., and Taylor, S. S. (1997) Identification of a novel protein kinase A anchoring protein that binds both type I and type II regulatory subunits. *J. Biol. Chem. 272*, 8057−8064.

(12) Aye, T. T., Soni, S., van Veen, T. A., van der Heyden, M. A., Cappadona, S., Varro, A., de Weger, R. A., de Jonge, N., Vos, M. A., Heck, A. J., and Scholten, A. (2012) Reorganized PKA-AKAP associations in the failing human heart. *J. Mol. Cell. Cardiol. 52*, 511−518.

(13) Margarucci, L., Roest, M., Preisinger, C., Bleijerveld, O. B., van Holten, T. C., Heck, A. J., and Scholten, A. (2011) Collagen stimulation of platelets induces a rapid spatial response of cAMP and cGMP signaling scaffolds. *Mol. BioSyst. 7*, 2311−2319.

(14) Burgers, P. P., Ma, Y., Margarucci, L., Mackey, M., van der Heyden, M. A., Ellisman, M., Scholten, A., Taylor, S. S., and Heck, A. J. (2012) A small novel A-kinase anchoring protein (AKAP) that localizes specifically protein kinase A-regulatory subunit I (PKA-RI) to the plasma membrane. *J. Biol. Chem. 287*, 43789−43797.

(15) Kovanich, D., van der Heyden, M. A., Aye, T. T., van Veen, T. A., Heck, A. J., and Scholten, A. (2010) Sphingosine kinase interacting protein is an A-kinase anchoring protein specific for type I cAMP-dependent protein kinase. *ChemBioChem 11*, 963−971.

(16) Means, C. K., Lygren, B., Langeberg, L. K., Jain, A., Dixon, R. E., Vega, A. L., Gold, M. G., Petrosyan, S., Taylor, S. S., Murphy, A. N., Ha, T., Santana, L. F., Tasken, K., and Scott, J. D. (2011) An entirely specific type I A-kinase anchoring protein that can sequester two molecules of protein kinase A at mitochondria. *Proc. Natl. Acad. Sci. U.S.A. 108*, E1227−E1235.

(17) Shanks, M. O., Lund, L. M., Manni, S., Russell, M., Mauban, J. R., and Bond, M. (2012) Chromodomain helicase binding protein 8 (Chd8) is a novel A-kinase anchoring protein expressed during rat cardiac development. *PLoS One 7*, e46316.

(18) Hundsrucker, C., Skroblin, P., Christian, F., Zenn, H. M., Popara, V., Joshi, M., Eichhorst, J., Wiesner, B., Herberg, F. W., Reif, B., Rosenthal, W., and Klussmann, E. (2010) Glycogen synthase kinase 3β interaction protein functions as an A-kinase anchoring protein. *J. Biol. Chem. 285*, 5507−5521.

(19) Carr, D. W., Stofko-Hahn, R. E., Fraser, I. D., Bishop, S. M., Acott, T. S., Brennan, R. G., and Scott, J. D. (1991) Interaction of the regulatory subunit (RII) of cAMP-dependent protein kinase with RII-anchoring proteins occurs through an amphipathic helix binding motif. *J. Biol. Chem. 266*, 14188−14192.

(20) Newlon, M. G., Roy, M., Hausken, Z. E., Scott, J. D., and Jennings, P. A. (1997) The A-kinase anchoring domain of type IIα cAMP-dependent protein kinase is highly helical. *J. Biol. Chem. 272*, 23637−23644.

(21) Sarma, G. N., Kinderman, F. S., Kim, C., von Daake, S., Chen, L., Wang, B. C., and Taylor, S. S. (2010) Structure of D-AKAP2:PKA RI complex: Insights into AKAP specificity and selectivity. *Structure 18*, 155−166.

(22) Gold, M. G., Lygren, B., Dokurno, P., Hoshi, N., McConnachie, G., Tasken, K., Carlson, C. R., Scott, J. D., and Barford, D. (2006) Molecular basis of AKAP specificity for PKA regulatory subunits. *Mol. Cell 24*, 383−395.

(23) Newlon, M. G., Roy, M., Morikis, D., Hausken, Z. E., Coghlan, V., Scott, J. D., and Jennings, P. A. (1999) The molecular basis for protein kinase A anchoring revealed by solution NMR. *Nat. Struct. Biol. 6*, 222−227.

(24) Burns-Hamuro, L. L., Ma, Y., Kammerer, S., Reineke, U., Self, C., Cook, C., Olson, G. L., Cantor, C. R., Braun, A., and Taylor, S. S.

(2003) Designing isoform-specific peptide disruptors of protein kinase A localization. *Proc. Natl. Acad. Sci. U.S.A. 100*, 4072−4077.
(25) Peng, M., Scholten, A., Heck, A. J., and van Breukelen, B. (2014) Identification of enriched PTM crosstalk motifs from large-scale experimental data sets. *J. Proteome Res. 13*, 249−259.
(26) Hamuro, Y., Burns, L., Canaves, J., Hoffman, R., Taylor, S., and Woods, V. (2002) Domain organization of D-AKAP2 revealed by enhanced deuterium exchange-mass spectrometry (DXMS). *J. Mol. Biol. 321*, 703−714.
(27) Dong, F., Feldmesser, M., Casadevall, A., and Rubin, C. S. (1998) Molecular characterization of a cDNA that encodes six isoforms of a novel murine A kinase anchor protein. *J. Biol. Chem. 273*, 6533−6541.
(28) Vijayaraghavan, S., Liberty, G. A., Mohan, J., Winfrey, V. P., Olson, G. E., and Carr, D. W. (1999) Isolation and molecular characterization of AKAP110, a novel, sperm-specific protein kinase A-anchoring protein. *Mol. Endocrinol. 13*, 705−717.
(29) Miki, K., and Eddy, E. M. (1998) Identification of tethering domains for protein kinase A type Iα regulatory subunits on sperm fibrous sheath protein FSC1. *J. Biol. Chem. 273*, 34384−34390.
(30) Kapiloff, M. S., Schillace, R. V., Westphal, A. M., and Scott, J. D. (1999) mAKAP: An A-kinase anchoring protein targeted to the nuclear membrane of differentiated myocytes. *J. Cell Sci. 112* (Part 16), 2725−2736.
(31) McCartney, S., Little, B. M., Langeberg, L. K., and Scott, J. D. (1995) Cloning and characterization of A-kinase anchor protein 100 (AKAP100). A protein that targets A-kinase to the sarcoplasmic reticulum. *J. Biol. Chem. 270*, 9327−9333.
(32) Fraser, I. D., Tavalin, S. J., Lester, L. B., Langeberg, L. K., Westphal, A. M., Dean, R. A., Marrion, N. V., and Scott, J. D. (1998) A novel lipid-anchored A-kinase anchoring protein facilitates cAMP-responsive membrane events. *EMBO J. 17*, 2261−2272.
(33) Brown, R. L., August, S. L., Williams, C. J., and Moss, S. B. (2003) AKAP7γ is a nuclear RI-binding AKAP. *Biochem. Biophys. Res. Commun. 306*, 394−401.
(34) Eide, T., Coghlan, V., Orstavik, S., Holsve, C., Solberg, R., Skalhegg, B. S., Lamb, N. J., Langeberg, L., Fernandez, A., Scott, J. D., Jahnsen, T., and Tasken, K. (1998) Molecular cloning, chromosomal localization, and cell cycle-dependent subcellular distribution of the A-kinase anchoring protein, AKAP95. *Exp. Cell Res. 238*, 305−316.
(35) Witczak, O., Skalhegg, B. S., Keryer, G., Bornens, M., Tasken, K., Jahnsen, T., and Orstavik, S. (1999) Cloning and characterization of a cDNA encoding an A-kinase anchoring protein located in the centrosome, AKAP450. *EMBO J. 18*, 1858−1868.
(36) Reinton, N., Collas, P., Haugen, T. B., Skalhegg, B. S., Hansson, V., Jahnsen, T., and Tasken, K. (2000) Localization of a novel human A-kinase-anchoring protein, hAKAP220, during spermatogenesis. *Dev. Biol. 223*, 194−204.
(37) Nauert, J. B., Klauck, T. M., Langeberg, L. K., and Scott, J. D. (1997) Gravin, an autoantigen recognized by serum from myasthenia gravis patients, is a kinase scaffold protein. *Curr. Biol. 7*, 52−62.
(38) Diviani, D., Soderling, J., and Scott, J. D. (2001) AKAP-Lbc anchors protein kinase A and nucleates Gα 12-selective Rho-mediated stress fiber formation. *J. Biol. Chem. 276*, 44247−44257.
(39) Kultgen, P. L., Byrd, S. K., Ostrowski, L. E., and Milgram, S. L. (2002) Characterization of an A-kinase anchoring protein in human ciliary axonemes. *Mol. Biol. Cell 13*, 4156−4166.
(40) Jarnaess, E., Stokka, A. J., Kvissel, A. K., Skalhegg, B. S., Torgersen, K. M., Scott, J. D., Carlson, C. R., and Tasken, K. (2009) Splicing factor arginine/serine-rich 17A (SFRS17A) is an A-kinase anchoring protein that targets protein kinase A to splicing factor compartments. *J. Biol. Chem. 284*, 35154−35164.
(41) Lim, C. J., Han, J., Yousefi, N., Ma, Y., Amieux, P. S., McKnight, G. S., Taylor, S. S., and Ginsberg, M. H. (2007) α4 integrins are type I cAMP-dependent protein kinase-anchoring proteins. *Nat. Cell Biol. 9*, 415−421.
(42) Diviani, D., Langeberg, L. K., Doxsey, S. J., and Scott, J. D. (2000) Pericentrin anchors protein kinase A at the centrosome through a newly identified RII-binding domain. *Curr. Biol. 10*, 417−420.
(43) Li, H., Adamik, R., Pacheco-Rodriguez, G., Moss, J., and Vaughan, M. (2003) Protein kinase A-anchoring (AKAP) domains in brefeldin A-inhibited guanine nucleotide-exchange protein 2 (BIG2). *Proc. Natl. Acad. Sci. U.S.A. 100*, 1627−1632.
(44) Ruppelt, A., Mosenden, R., Gronholm, M., Aandahl, E. M., Tobin, D., Carlson, C. R., Abrahamsen, H., Herberg, F. W., Carpen, O., and Tasken, K. (2007) Inhibition of T cell activation by cyclic adenosine 5′-monophosphate requires lipid raft targeting of protein kinase A type I by the A-kinase anchoring protein ezrin. *J. Immunol. 179*, 5159−5168.
(45) Dransfield, D. T., Bradford, A. J., Smith, J., Martin, M., Roy, C., Mangeat, P. H., and Goldenring, J. R. (1997) Ezrin is a cyclic AMP-dependent protein kinase anchoring protein. *EMBO J. 16*, 35−43.
(46) Semenova, I., Ikeda, K., Ivanov, P., and Rodionov, V. (2009) The protein kinase A-anchoring protein moesin is bound to pigment granules in melanophores. *Traffic 10*, 153−160.
(47) Schillace, R. V., Andrews, S. F., Liberty, G. A., Davey, M. P., and Carr, D. W. (2002) Identification and characterization of myeloid translocation gene 16b as a novel a kinase anchoring protein in T lymphocytes. *J. Immunol. 168*, 1590−1599.
(48) Uys, G. M., Ramburan, A., Loos, B., Kinnear, C. J., Korkie, L. J., Mouton, J., Riedemann, J., and Moolman-Smook, J. C. (2011) Myomegalin is a novel A-kinase anchoring protein involved in the phosphorylation of cardiac myosin binding protein C. *BMC Cell Biol. 12*, 18.
(49) Roder, I. V., Choi, K. R., Reischl, M., Petersen, Y., Diefenbacher, M. E., Zaccolo, M., Pozzan, T., and Rudolf, R. (2010) Myosin Va cooperates with PKA RIα to mediate maintenance of the endplate in vivo. *Proc. Natl. Acad. Sci. U.S.A. 107*, 2031−2036.
(50) Kussel-Andermann, P., El-Amraoui, A., Safieddine, S., Hardelin, J. P., Nouaille, S., Camonis, J., and Petit, C. (2000) Unconventional myosin VIIA is a novel A-kinase-anchoring protein. *J. Biol. Chem. 275*, 29654−29659.
(51) Reynolds, J. G., McCalmon, S. A., Tomczyk, T., and Naya, F. J. (2007) Identification and mapping of protein kinase A binding sites in the costameric protein myospryn. *Biochim. Biophys. Acta 1773*, 891−902.
(52) Goehring, A. S., Pedroja, B. S., Hinke, S. A., Langeberg, L. K., and Scott, J. D. (2007) MyRIP anchors protein kinase A to the exocyst complex. *J. Biol. Chem. 282*, 33155−33167.
(53) Wang, X., Herberg, F. W., Laue, M. M., Wullner, C., Hu, B., Petrasch-Parwez, E., and Kilimann, M. W. (2000) Neurobeachin: A protein kinase A-anchoring, beige/Chediak-higashi protein homolog implicated in neuronal membrane traffic. *J. Neurosci. 20*, 8551−8565.
(54) Li, H., Degenhardt, B., Tobin, D., Yao, Z. X., Tasken, K., and Papadopoulos, V. (2001) Identification, localization, and function in steroidogenesis of PAP7: A peripheral-type benzodiazepine receptor- and PKA (RIα)-associated protein. *Mol. Endocrinol. 15*, 2211−2228.
(55) Alto, N. M., Soderling, J., and Scott, J. D. (2002) Rab32 is an A-kinase anchoring protein and participates in mitochondrial dynamics. *J. Cell Biol. 158*, 659−668.
(56) Jivan, A., Earnest, S., Juang, Y. C., and Cobb, M. H. (2009) Radial spoke protein 3 is a mammalian protein kinase A-anchoring protein that binds ERK1/2. *J. Biol. Chem. 284*, 29437−29445.
(57) Russell, M. A., Lund, L. M., Haber, R., McKeegan, K., Cianciola, N., and Bond, M. (2006) The intermediate filament protein, synemin, is an AKAP in the heart. *Arch. Biochem. Biophys. 456*, 204−215.
(58) Westphal, R. S., Soderling, S. H., Alto, N. M., Langeberg, L. K., and Scott, J. D. (2000) Scar/WAVE-1, a Wiskott-Aldrich syndrome protein, assembles an actin-associated multi-kinase scaffold. *EMBO J. 19*, 4589−4600.
(59) Yamashita, H., Ueda, K., and Kioka, N. (2011) WAVE2 forms a complex with PKA and is involved in PKA enhancement of membrane protrusions. *J. Biol. Chem. 286*, 3907−3914.
(60) Petersen, B., Petersen, T. N., Andersen, P., Nielsen, M., and Lundegaard, C. (2009) A generic method for assignment of reliability

scores applied to solvent accessibility predictions. *BMC Struct. Biol. 9*, 51.
(61) Zhong, W., Zhou, Y., Li, S., Zhou, T., Ma, H., Wei, K., Li, H., Olkkonen, V. M., and Yan, D. (2011) OSBP-related protein 7 interacts with GATE-16 and negatively regulates GS28 protein stability. *Exp. Cell Res. 317*, 2353−2363.
(62) Skaff, D. A., Kim, C. S., Tsai, H. J., Honzatko, R. B., and Fromm, H. J. (2005) Glucose 6-phosphate release of wild-type and mutant human brain hexokinases from mitochondria. *J. Biol. Chem. 280*, 38403−38409.
(63) de Vries, S. J., van Dijk, A. D., Krzeminski, M., van Dijk, M., Thureau, A., Hsu, V., Wassenaar, T., and Bonvin, A. M. (2007) HADDOCK versus HADDOCK: New features and performance of HADDOCK2.0 on the CAPRI targets. *Proteins 69*, 726−733.
(64) Dominguez, C., Boelens, R., and Bonvin, A. M. (2003) HADDOCK: A protein-protein docking approach based on biochemical or biophysical information. *J. Am. Chem. Soc. 125*, 1731−1737.
(65) Scholten, A., Poh, M. K., van Veen, T. A., van Breukelen, B., Vos, M. A., and Heck, A. J. (2006) Analysis of the cGMP/cAMP interactome using a chemical proteomics approach in mammalian heart tissue validates sphingosine kinase type 1-interacting protein as a genuine and highly abundant AKAP. *J. Proteome Res. 5*, 1435−1447.
(66) Scholten, A., van Veen, T. A., Vos, M. A., and Heck, A. J. (2007) Diversity of cAMP-dependent protein kinase isoforms and their anchoring proteins in mouse ventricular tissue. *J. Proteome Res. 6*, 1705−1717.
(67) Lubsen, N. H., Aarts, H. J., and Schoenmakers, J. G. (1988) The evolution of lenticular proteins: The β- and γ-crystallin super gene family. *Prog. Biophys. Mol. Biol. 51*, 47−76.
(68) Chen, Z., Borek, D., Padrick, S. B., Gomez, T. S., Metlagel, Z., Ismail, A. M., Umetani, J., Billadeau, D. D., Otwinowski, Z., and Rosen, M. K. (2010) Structure and control of the actin regulatory WAVE complex. *Nature 468*, 533−538.
(69) Herberg, F. W., Maleszka, A., Eide, T., Vossebein, L., and Tasken, K. (2000) Analysis of A-kinase anchoring protein (AKAP) interaction with protein kinase A (PKA) regulatory subunits: PKA isoform specificity in AKAP binding. *J. Mol. Biol. 298*, 329−339.